

Dynamics of density imbalanced bilayer holes in the quantum Hall regime

S. Misra, N. C. Bishop, E. Tutuc,^{*} and M. Shayegan*Department of Electrical Engineering, Princeton University, Princeton, New Jersey 08544, USA*

(Received 15 April 2008; published 21 July 2008)

We report magnetotransport measurements on bilayer GaAs hole systems with unequal hole concentrations in the two layers. At magnetic fields where one layer is in the integer quantum Hall state and the other has bulk extended states at the Fermi energy, the longitudinal and the Hall resistances of the latter are hysteretic, in agreement with previous measurements. For a fixed magnetic field inside this region and at low temperatures ($T \leq 350$ mK), the time evolutions of the longitudinal and Hall resistances show pronounced jumps followed by slow relaxations, with no end to the sequence of jumps. Our measurements demonstrate that the jumps occur simultaneously in pairs of contacts $170\ \mu\text{m}$ apart and appear to involve changes in the charge configuration of the bilayer. In addition, the jumps can occur with either random or regular periods, excluding thermal fluctuations as a possible origin for the jumps. Finally, while remaining at a fixed field, we warm the sample to above 350 mK, where the jumps disappear. Upon recooling the sample below this temperature, the jumps reappear, indicating that the jumps do not result from nearly dissipationless eddy currents either.

DOI: [10.1103/PhysRevB.78.035322](https://doi.org/10.1103/PhysRevB.78.035322)

PACS number(s): 73.21.-b, 73.43.-f, 73.50.Td

I. INTRODUCTION

The hallmarks of the integer quantum Hall effect, a quantized Hall resistance and zero longitudinal resistance in two-dimensional (2D) carrier systems at low temperatures, are essentially independent of the sample characteristics. This universal behavior results from the Fermi energy lying in between two Landau levels (LLs), meaning that the bulk has only localized states at the Fermi energy, and thus the sample's properties are dominated by the extended one-dimensional edge states.¹ Accordingly, the properties of the bulk have been difficult to access directly except in a series of recent scanning probe experiments.²⁻⁴ These studies indicate that the bulk can be thought of as a set of isolated quantum dots and antidots separated by incompressible regions.

A number of recent experiments have placed a probe such as a single electron transistor,⁵ a magnetometer,^{6,7} or even another conducting 2D layer,⁸⁻¹¹ close to a 2D layer in the quantum Hall state (QHS) to explore how the isolated bulk states achieve equilibrium. Here we focus on a bilayer 2D hole system with unequal hole densities such that, at a particular magnetic field, the Fermi energy lies in between LLs for one layer and near the middle of one LL for the other layer. In samples with narrow tunnel barriers between the two layers ($w_b < 7.5$ nm), the holes can easily tunnel between the two layers and the system appears to be in equilibrium.⁹ In contrast, for samples with wider barriers ($w_b > 7.5$ nm), the magnetoresistance of the conducting layer, which we call the probe layer, is hysteretic for the range of magnetic fields where the other layer is in a QHS (Refs. 8–11). This effect has been proposed to be the consequence of a nonequilibrium charge distribution.^{8,9,11} The charge configurations of the QHS layer are different on the low-field and high-field sides of the QHS, which result in different charge configurations for the probe layer as well. This charge configuration becomes frozen once the former enters the QHS, resulting in a hysteretic magnetoresistance. For bilayer hole samples with intermediate barrier widths

($7.5\ \text{nm} < w_b < 200\ \text{nm}$), once the magnetic field is set such that one layer is in the QHS, the system appears to never reach equilibrium. Instead, both the longitudinal and the Hall resistances of the probe layer show large jumps as a function of time: the resistance changes by $\Delta r \sim 50\text{--}500\ \Omega$ over a short time (faster than 300 ms), typically followed by a slow relaxation ($\tau \sim 40\text{--}400$ s) with no apparent end to the sequence of jumps.⁹

The purpose of this paper is to present data describing additional features of this nonequilibrium phenomenon. Section II covers the details of the experiment. In Sec. III, we demonstrate that the resistance jumps occur simultaneously in pairs of contacts, which are $170\ \mu\text{m}$ apart, and appear to involve a change in the charge configuration of the bilayer. We show in Sec. IV that the jumps can occur at quasiperiodic time intervals or, for slightly different experimental conditions, at largely random time intervals. Data presented in Sec. V reveal that the jumps decrease in amplitude with increasing temperature and disappear above ~ 350 mK. Surprisingly, when we recool the sample in a fixed magnetic field, the jumps reappear at low temperatures. In Sec. VI, we conclude with a discussion of possible physical explanations of the data.

II. EXPERIMENT DETAILS

We performed electrical transport measurements on double quantum well samples grown on GaAs (311)A substrates. Although the behavior described here has been observed for a number of hole bilayer samples having a range of barrier thicknesses and densities,⁹ we present data taken on three samples from one wafer. The wafer contains a pair of 15-nm-wide GaAs quantum wells separated by a $w_b = 11$ nm AlAs barrier and flanked by a spacer and Si-doped layers of $\text{Al}_{0.21}\text{Ga}_{0.79}\text{As}$. Sample A consists of a Hall bar with two current arms and six voltage probe arms, with an active region of $100 \times 900\ \mu\text{m}^2$, as illustrated schematically in the inset to Fig. 1(a). The distance between two adjacent contacts on one side is $170\ \mu\text{m}$, and the width of the Hall bar is

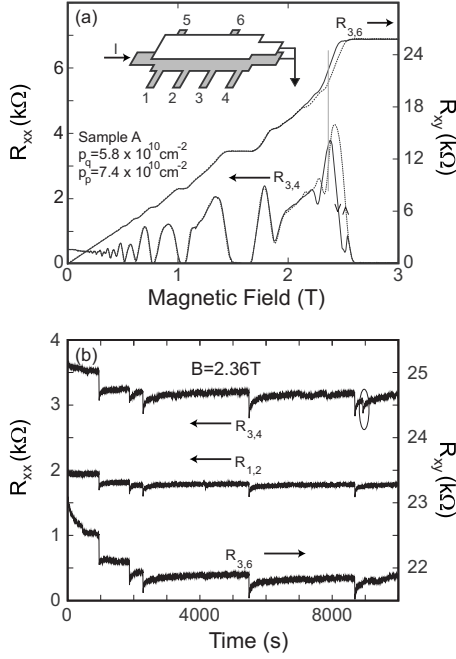


FIG. 1. For sample A, we adopt the convention that $R_{i,j}$ refers to the resistance measured between contacts i and j of the Hall bar (inset). (a) The longitudinal ($R_{3,4}$) and the Hall ($R_{3,6}$) resistances of the probe layer are hysteretic for a range of fields where the other layer is in the QHS. The densities of the QHS and probe layers are given by p_q and p_p , respectively. (b) The time evolution of the longitudinal resistances, $R_{1,2}$ and $R_{3,4}$, and the Hall resistance $R_{3,6}$ taken simultaneously after sweeping the magnetic field up to 2.36 T, indicated by a vertical line in (a). The circled jump is the only one which does not occur simultaneously in all contact pairs.

100 μm . Samples B and C have simpler Hall bar configurations, with a pair of current contacts and two voltage contacts. Alloyed InZn contacts were used to contact both layers of the structure. Using a selective gate-depletion scheme,¹² we could also independently contact the bottom layer in sample A or either layer in sample C.

Electrical transport measurements were made at a temperature of 30 mK, unless otherwise noted, using standard ac lock-in techniques with a drive current of 1 nA at a frequency of 4.2 Hz. The as-grown densities for the three samples used in this paper are $8 \times 10^{10} \text{ cm}^{-2}$ (top layer) and $6 \times 10^{10} \text{ cm}^{-2}$ (bottom layer), and the typical mobility at 30 mK is $\approx 30 \text{ m}^2/\text{Vs}$. In order to determine the carrier densities of the two layers in sample A, we compared the total density to the density of just the bottom layer, both extracted from the Hall resistance (R_{xy}) at low magnetic fields. In sample B, we examined the Shubnikov–de Haas oscillations of the longitudinal resistance (R_{xx}) of the bilayer in order to determine the densities of the top and bottom layers. For sample C, we compared the Shubnikov–de Haas oscillations of R_{xx} of the top and the bottom layers, acquired independently, to establish the carrier densities of the two layers. The density of the bottom layer was then set such that it had a filling factor ν in between one and two at a magnetic field where the top layer had a filling factor $\nu=1$. Thus, the Fermi energy of the bottom layer is in the second LL for a range of fields where the Fermi energy of the top layer is in between

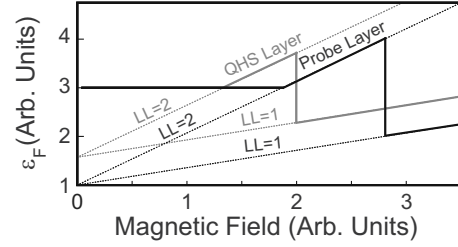


FIG. 2. Schematic diagram of the change in the Fermi energy as a function of magnetic field for the probe layer (black) and the QHS layer (gray), referenced to the Fermi energy of the respective layer at zero magnetic field. Also shown as dotted lines are the energies of the first and second LLs for both layers.

the first and second LLs. Unless noted otherwise, we report on the resistance of just the bottom layer, which we refer to as the probe layer, while the other layer (which we refer to as the QHS layer) is held at ground using a common ground contact. For sample B, we show the resistance of the bilayer, which is indicative of the resistance of the probe layer. At magnetic fields where the QHS layer is near $\nu=1$, current flowing through this layer causes no drop in longitudinal voltage. As a result, the voltage drop sensed across two *bi-layer* longitudinal contacts occurs solely in the probe layer.

III. LAYER CHARGE INSTABILITY

Figure 1(a) shows the magnetoresistance of the probe layer of sample A at 30 mK, when the *probe* layer has a density $p_p = 7.4 \times 10^{10} \text{ cm}^{-2}$ and the other (*QHS*) layer has a density $p_q = 5.8 \times 10^{10} \text{ cm}^{-2}$. As seen in this figure, the probe layer exhibits the zero longitudinal resistance and the quantized Hall resistance characteristic of the integer quantum Hall effect. In addition, both the longitudinal and the Hall resistances of the probe layer are seen to be hysteretic in the range of magnetic fields where the other layer is in the $\nu=1$ QHS. The hysteresis is consistent with earlier reports from a single-well sample with an unintentional parasitic layer⁸ and with recent measurements of intentionally imbalanced bilayer hole⁹ and electron^{10,11} samples.

This hysteresis is believed to result from a nonequilibrium interlayer charge distribution.^{8,9,11} This can be understood by examining how the Fermi energy of two layers changes as a function of the magnetic field, as illustrated schematically in Fig. 2. Because the probe layer has a larger density than the QHS layer at zero magnetic field, we show the bottom of the subbands for the two wells as being offset from one another but the Fermi energies as being equal (at zero magnetic field). Upon increasing the magnetic field just below the point where the QHS layer is at filling factor $\nu=1$, the Fermi energy of this layer has increased more than that of the probe layer. This results in a redistribution of charge between the two layers, such that the QHS layer will have a higher carrier density relative to what it had at zero magnetic field, and the probe layer will have a lower density. By the same argument, upon *decreasing* the magnetic field to just above the point where the QHS layer is at $\nu=1$, its Fermi energy has decreased relative to what it was at zero magnetic field. Thus,

the QHS layer will have a lower carrier density relative to what it had at zero magnetic field, and the probe layer will have a higher density. Upon entering the QHS, the charge configuration of the QHS layer becomes frozen, as there are now only localized states at the Fermi energy, and large incompressible regions separate these states from a reservoir. This layer exerts an electrostatic potential on the probe layer, and thus the density of the latter becomes trapped at a non-equilibrium level as well. Because its density is lower (higher) than at zero magnetic field when sweeping the magnetic field up (down), the magnetoresistance of the probe layer should look shifted to lower (higher) fields, consistent with the data shown in Fig. 1(a). At even higher magnetic fields, the Fermi energy of the QHS layer will remain in the first LL, while the probe layer will enter the $\nu=1$ QHS; that is, their roles reverse. Just below the field where the probe layer enters the $\nu=1$ QHS, it has a higher Fermi energy than the QHS layer. Just above the field where it enters the $\nu=1$ QHS, it has a lower Fermi energy than the QHS layer. This situation is thus identical to the one described above, and thus, we would expect the magnetoresistance of the QHS layer to look shifted to lower (higher) fields when sweeping the magnetic field up (down). Note in particular that this picture is also consistent with the data presented in Ref. 9. Finally, the hysteresis is seen in our samples only for the $\nu=1$ QHS, which is likely due to their comparatively low carrier density. In contrast, the hysteresis is seen for higher numbered LLs in higher-density samples by Ref. 8. This is likely a consequence of the strength of the QHS being a function of the magnetic field, and not the filling factor.

In agreement with the results reported in Ref. 9 for bilayer hole samples with intermediate barrier widths ($7.5 \text{ nm} < w_b < 200 \text{ nm}$), we find that the bilayer system shows peculiar dynamics in the hysteretic region of magnetic fields. As shown in Fig. 1(b), for example, the time evolution of the resistance after stopping a field sweep in the hysteretic region features sudden jump in resistance, where the resistance changes by $\Delta R \approx \pm 25$ to $\pm 500 \text{ } \Omega$ over a short time scale (as fast as 300 ms) that is limited by our experimental bandwidth. A jump is followed by a slow relaxation over a long time scale ($\tau \approx 20\text{--}400 \text{ s}$), and then another jump occurs a time ($\Delta t \approx 30\text{--}3000 \text{ s}$) later. This sequence of jumps continues for as long as we have tracked the time evolution, up to $\sim 10^5 \text{ s}$, with no systematic change in the jump amplitude or sign, the time spacing between jumps, or the relaxation-time constant. Consistent with previous results,⁹ we find that these characteristics depend sensitively on the magnetic field and carrier concentration and are different for separate cool downs. The data indicate that the dynamics of the sample itself are responsible for the jumps. No such jumps are seen in a resistor hooked up in series with the sample or when measuring the sample at a magnetic field outside the hysteretic region. None of the characteristics of the jumps change significantly when varying the drive current used to measure the resistance (0.5–8 nA), up to the point where the drive current starts to heat the sample. Most strikingly, the jumps happen whether or not we probe the resistance, as shown in Fig. 3. Even when grounding the sample for hundreds of seconds, and then resuming our measurement, we can see the decay associated with a jump, which must have happened while the sample was grounded.

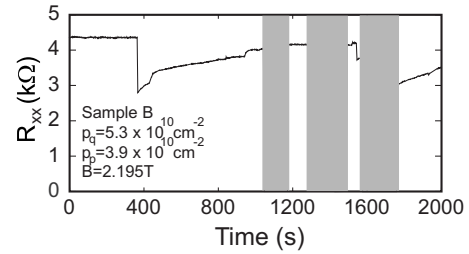


FIG. 3. The time evolution of the longitudinal resistance of the bilayer where the contacts to the sample are grounded for the time periods shown in gray. Note in particular that a jump must have occurred during the third time period, even though the sample was grounded.

The jumps themselves signal a significant change in the properties of the probe layer. In Fig. 4, we compare magnetoresistance traces taken from sample B when sweeping the magnetic field at two different sweep rates: one fast enough that no jumps occur while sweeping the field, and a second slow enough that many jumps occur. The fast magnetoresistance traces (dotted lines), which contain no jumps, define the two branches of the hysteresis loop: the upward and downward branches. When sweeping the magnetic field slowly enough so that the resistance does jump during the field sweep (solid line), we find that the magnetoresistance trace departs from the branch of the hysteresis loop on which it would be expected to lie. For the data in Fig. 4, when we slowly sweep the magnetic field up, we find that the jumps first cause this magnetoresistance trace to depart from the upward branch of the hysteresis loop to a point where the magnetoresistance is not even at a value in between the extremes defined by the upward and downward branches of the hysteresis loop. Later, further jumps result in the magnetoresistance joining the *downward* branch of the hysteresis loop despite being taken while sweeping the magnetic field *upward*. Although it is more common that jumps shift the magnetoresistance to curves unrelated to the upward or downward branch of the hysteresis loop, these data clearly demonstrate that the jumps have changed the carrier concen-

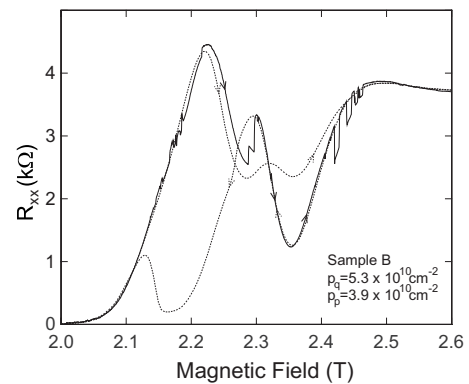


FIG. 4. Solid trace: the longitudinal magnetoresistance of the bilayer taken while sweeping the magnetic field up at a rate of 0.17 mT/s. Dotted traces: magnetoresistance of the bilayer while sweeping the field at a rate of 3.3 mT/s in the direction indicated by the arrows.

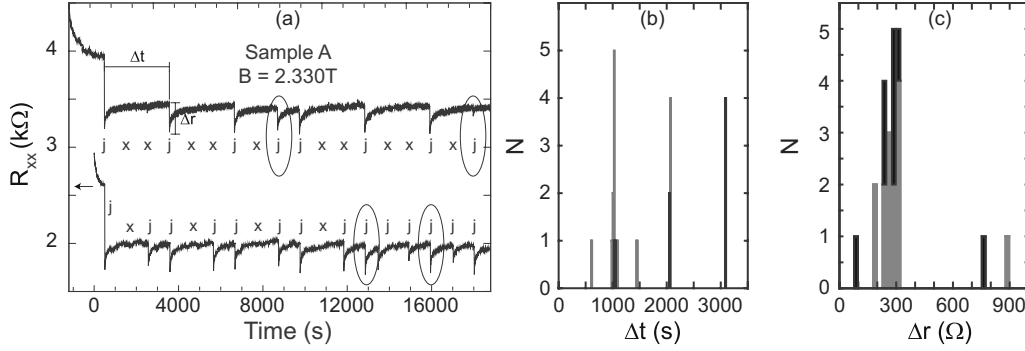


FIG. 5. (a) Time evolution of $R_{1,3}$ for the probe layer of sample A taken immediately after ramping the magnetic field from 0 T up to 2.33 T. The layer densities are $p_p = 7.4 \times 10^{10} \text{ cm}^{-2}$ and $p_q = 5.8 \times 10^{10} \text{ cm}^{-2}$. The experiment was repeated twice, and the two sets of time evolution data have been offset vertically for clarity and horizontally to match the position of the first jump. (b) Stacked histogram of the time Δt between consecutive jumps in the time captures shown in (a), with black (gray) bars corresponding to Δt extracted from the top (bottom) trace. Taking the basic time block to be 1030 s, the train of jumps in the top trace of part (a) follows the sequence jump (j), no jump (x), no jump (x), with two jumps occurring out of sequence (circled). The train of jumps for the bottom time capture shown in part (a) follows the sequence j - x - j , with two extra jumps occurring out of sequence (circled). The first of the circled jumps in the lower trace of (a) is the only one whose Δt is not an integer multiple of 1030 s. (c) Stacked histogram of the size of a resistance jump Δr . Excluding the jump that starts the sequence, the standard deviation of jumps sizes (55 Ω) is much smaller than the median jump size (285 Ω).

tration of the probe layer. Within the layer charge instability scenario, the data would suggest that there are a number of bilayer charge configurations, which produce different magnetoresistance curves. These magnetoresistance curves have similar features, but appear shifted in magnetic field, suggesting that these charge configurations involve different carrier concentrations for the probe layer. The jumps seen in, for example, Fig. 1(b), would thus result from sudden changes in the probe layer charge configuration.

We next address whether these jumps are local fluctuations of the charge configuration by measuring the resistance simultaneously in three sets of contacts. As shown in Fig. 1(b), we find that the jumps almost always occur at the same time in all three sets of contacts, which are up to 170 μm apart. This indicates that the jumps are not the result of a local fluctuation and implies that there is a change in either the QHS layer or the probe layer over large length scales, which is responsible for creating a jump in the probe layer resistance. However, the direction and amplitude of the jumps, and the relaxation-time constant, are not (in general) the same for the jumps seen simultaneously in different contacts. We also occasionally observe a jump in only one of the longitudinal sets of contacts, or in the Hall contacts, without any jump in the other two sets of contacts. These observations suggest that the charge configuration is changing over a length scale, which, while large, does not extend across the entire sample.

IV. QUASIPERIODIC OSCILLATIONS

Thermal fluctuations are the most obvious candidates for what drives the imbalanced bilayer to jump between various charge configurations. The physical situation where a system has two nearly energy degenerate charge configurations in a quantizing magnetic field has been studied previously in resonant transport through a quantum dot.^{13,14} In these studies, the quantum dot has two charge configurations with

similar energies, one which has a high conductance and the other a low conductance. The fluctuations in the charge configuration of the quantum dot result in a conductance which switches between the high and low values to create telegraph noise. As is to be expected for a process driven by fluctuations, the amount of time between switching events is rather widely distributed.

In order to determine whether fluctuations are responsible for the jumps in resistance seen in our imbalanced bilayer system, we examine the distribution of time elapsed in between jumps. In Fig. 5(a), we show the time evolution of the resistance taken immediately after sweeping the magnetic field into the hysteretic range of fields and stopping at a particular field. Each of the two time evolutions shown in Fig. 5(a) were recorded after ramping the magnetic field from 0 to 2.33 T, and then recording R_{xx} as a function of time. As shown in Fig. 5(b), the time elapsed between successive jumps, Δt , is not widely distributed but rather is almost always either 1030 ± 40 s, 2060 ± 10 s, or 3090 ± 5 s. Reexamining Fig. 5(a) data in blocks of 1030 s periods, the top trace shows a jump (j), followed by no jump (x), and then again by no jump (x). This j - x - x pattern repeats every 3090 s. The bottom trace shows a j - x - j pattern, which repeats every 3090 s. In all cases, this pattern becomes less robust the longer we take the data, although the quasiperiodicity remains. Comparing the two traces and shifting them in time so that their first jump lines up [as shown in Fig. 5(a)] reveals that all eight jumps seen in the top trace occur within 20 s of a jump in the bottom trace. Combined, these observations indicate the presence of a reliable time scale for the jumps, and thus exclude the possibility that thermal fluctuations are driving the system to switch between a set of nearly energy degenerate charge configurations. The distribution of resistance jump amplitudes [shown in Fig. 5(c)] is relatively sharp, in as much as the standard deviation of jump sizes (55 Ω) is much smaller than the median jump size (285 Ω).

The quasiperiodic behavior of jumps seen in Fig. 5, however, is not always observed. In the time evolution data for

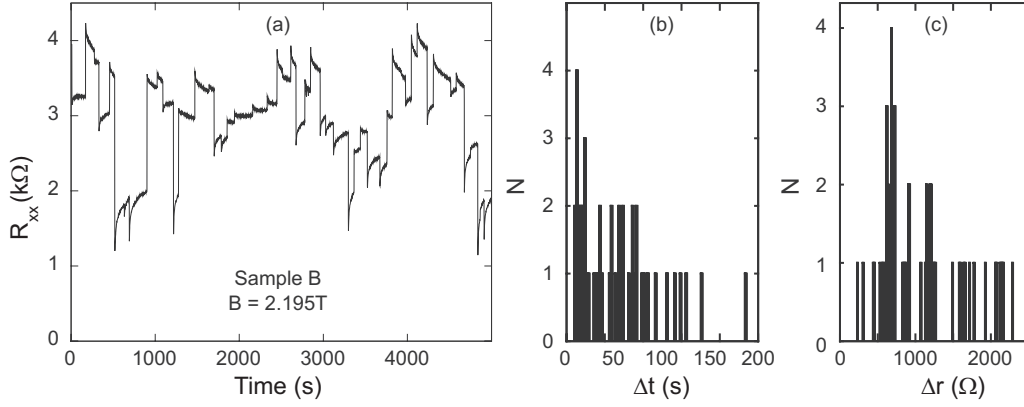


FIG. 6. (a) The time evolution of sample B, having layer densities of $p_p = 5.3 \times 10^{10} \text{ cm}^{-2}$ and $p_q = 3.9 \times 10^{10} \text{ cm}^{-2}$. (b) Histogram of the time Δt between consecutive jumps in the time capture shown in (a). (c) Histogram of the size of a jump Δr . The standard deviation of jump sizes (500 Ω) is nearly as large as the median (575 Ω).

sample B (Ref. 9), for example, shown in Fig. 6(a), the system appears to be jumping between a significantly larger number of quasistable points, as jumps occur in both directions, and do not appear to relax to the same value. The histogram of the time between jumps [shown in Fig. 6(b)] is not sharply peaked at a small number of values [as in Fig. 5(b)] but is rather widely distributed. Quantitatively, the distribution of jump amplitudes for the data in Fig. 6 is wide, as can be seen by comparing the standard deviation of jump amplitudes with the mean jump amplitude. Finally, we note that the occurrence of a semiregular period and a narrow distribution of jump sizes (as in Fig. 5), as opposed to a largely random period and wide distribution of jump sizes (as in Fig. 6), are not mutually exclusive. Curiously, even when the system has a wide range of jump amplitudes, it can exhibit quasiperiodic time evolution. In Figs. 7 and 8, which will be discussed in Sec. V, the system appears to be jumping between a number of quasistable points; the jumps relax to different values of resistance. Similar to the data shown in Fig. 5(b), and unlike the data in Fig. 6(b), the distribution of time between successive jumps shows quasiperiodic behavior. However, unlike the data in Fig. 5(c), and similar to the data in Fig. 6(c), the distribution of jump amplitudes is broad.

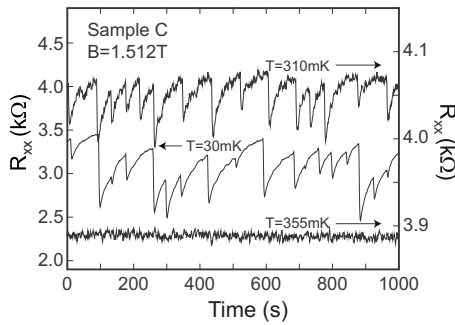


FIG. 7. Time evolution of the longitudinal resistance of the probe layer at 1.512 T in sample C, with layer densities of $p_p = 6.7 \times 10^{10} \text{ cm}^{-2}$ and $p_q = 4.1 \times 10^{10} \text{ cm}^{-2}$. Shown are representative of 1000 s slices of 5000-s long sweeps taken at 30, 310, and 355 mK.

V. TEMPERATURE DEPENDENCE

The nonequilibrium behavior of the probe layer is intimately tied to the other layer in the bilayer being in the $\nu = 1$ QHS. Because the strength of the QHS decreases with increasing temperature, we expect the properties of the jumps to change upon increasing the temperature of the system. In Figs. 7 and 8, we examine how the jumps change upon increasing the temperature for sample C. The magnetic

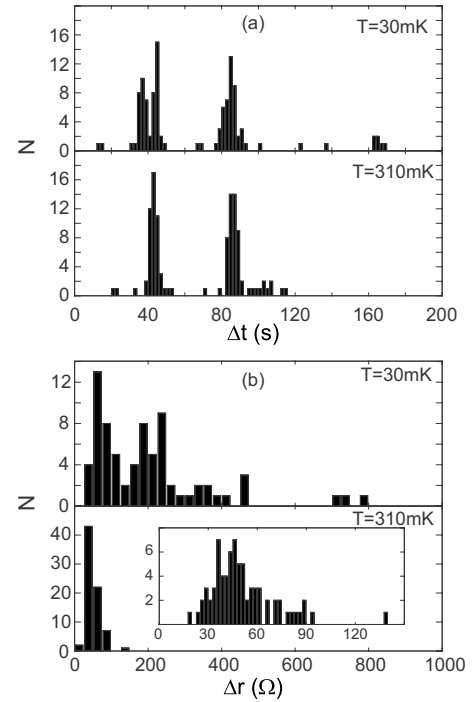


FIG. 8. Statistics for the jumps seen in the time evolution data shown in Fig. 7. (a) Histograms of the time Δt between consecutive jumps. (b) Histograms of the jump size Δr . The inset shows a magnified histogram of the 310 mK data. Note that we use a bin size of 25 Ω in the main part of (b), while we use a bin size of 2.5 Ω in the inset. Note also that all the histograms shown in this figure are for the entire, 5000-s long, traces whose 1000 s slices are shown in Fig. 7.

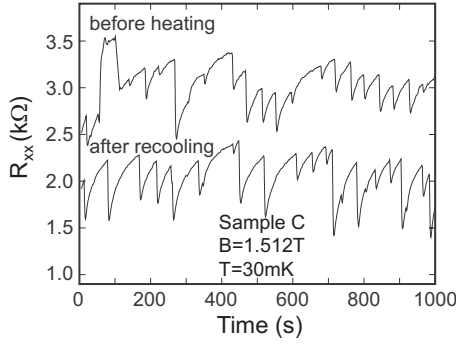


FIG. 9. Representative time evolution of the longitudinal resistance of the probe layer at 1.512 T in sample C. The top trace, which is a different 1000 s slice of the same 5000 s sweep used in Fig. 7, was first recorded at 30 mK. Then, with the magnetic field fixed at 1.512 T, the sample was heated to a temperature (355 mK) where the jumps disappear. We then recool the sample back to 30 mK and recorded the time evolution (1000 s of which is shown in the bottom trace) after reaching base temperature again.

field was first swept up to 1.512 T, and 5000 s elapsed before taking the first time evolution at $T=30$ mK (center trace in Fig. 7). While remaining at this field, we then warmed the sample up slowly, tracking the time evolution at a number of temperatures. We find that the jumps decrease in amplitude upon increasing the temperature but otherwise are qualitatively similar to how they appear at 30 mK. In Fig. 7 (upper trace), we show the time evolution at 310 mK—where the jumps are clearly visible, although their amplitude is significantly smaller than at 30 mK. As can be seen by examining the histogram of time between jumps [Fig. 8(a)], the quasiperiodic nature of the jumps at this field is unaffected by raising the temperature. What changes dramatically is the amplitude of the jumps [as shown in Fig. 8(b)], which drops from hundreds of ohms at 30 mK to tens of ohms at 310 mK. The time constant for the slow relaxation after a jump, determined by fitting the relaxation to a double exponential (as in Ref. 9), remains roughly 40 s at both temperatures. However, the temperature independence of the relaxation time seen here is not a robust feature of the data. For sample A, at a magnetic field of 1.87 T and layer densities of 5.1 and $7.4 \times 10^{10} \text{ cm}^{-2}$, the relaxation time was seen to vary between 400 s at a temperature of 30 mK and 10 s at 270 mK.

At high enough temperatures, the QHS layer begins to weakly conduct. At that point, any nonequilibrium condition induced by the field sweep should dissipate. We heated the sample above the temperature [355 mK, lower trace on Fig. 7(a)] where the jumps and the hysteresis in the probe layer magnetoresistance disappear, allowing the sample to come to equilibrium. In Figs. 9 and 10, we compare two sets of data taken at a fixed magnetic field; the first set before heating the sample, and the second after heating the sample to 355 mK and then cooling back to 30 mK over three hours. Surprisingly, when we recool the sample, the jumps in the time evolution resume. But the histogram of times in between jumps has also changed from being quasiperiodic to being nonperiodic after recooling.

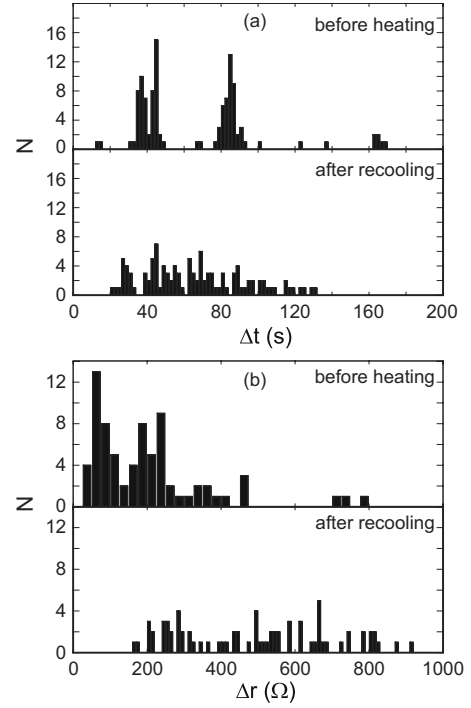


FIG. 10. Statistics for the jumps seen in the time evolution data shown in Fig. 9. (a) Histograms of the time Δt between consecutive jumps. (b) Histograms of the jump size Δr . Note that the same trace was analyzed for the “before heating” condition as was analyzed for the 30 mK data in Fig. 8.

VI. SUMMARY AND DISCUSSION

We have examined the magnetoresistance of bilayer hole systems whose layer densities have been intentionally set to be unequal. At magnetic fields where one layer is in the $\nu=1$ QHS and the other layer (the probe layer) has bulk extended states at the Fermi energy, the longitudinal and the Hall resistances of the latter are hysteretic, in agreement with previous studies.^{8–11} For a fixed magnetic field inside this hysteretic region, and at low temperatures, the resistance of the probe layer shows pronounced jumps followed by a slow relaxation with no end to the sequence of jumps, also in agreement with previous work.⁹ The data presented in Sec. III suggest that the probe layer resistance jumps in response to the system switching between different charge configurations. In addition, we have shown that the resistance jumps almost always occur simultaneously in pairs of contacts, which are $170 \text{ } \mu\text{m}$ apart, suggesting that the charge configuration of a significant part of the probe layer changes.

In Sec. IV, we have demonstrated that the jumps can occur at quasiperiodic time intervals or, for slightly different conditions, at largely random time intervals. The observation of quasiperiodic jumps excludes the possibility that the jumps represent thermal fluctuations between a set of nearly energy degenerate charge configurations, as such jumps would be expected to occur at random time intervals. The presence of a reproducible time scale for a cycle that includes a jump followed by a relaxation is a defining characteristic of relaxation oscillators. In a typical relaxation oscillator, a voltage builds up across a capacitor until a

breakdown threshold is exceeded, at which point the capacitor discharges. Such a behavior has been seen in a circuit containing a capacitor in parallel with a Corbino disk in the QHS (Ref. 15). In this system, the capacitor charges until the QHS breaks down, which leads to a discharging of the capacitor until the QHS in the Corbino disk can be established again. Relaxation oscillations have also been seen in the breakdown of the reentrant integer QHSs (Ref. 16) and in the transition from a pinned to a sliding Wigner solid phase.¹⁷ The presence of nonperiodic jumps is difficult to understand in terms of a single relaxation oscillator, which should always have a well-defined period. One possibility is that our system contains a number of relaxation oscillators in different parts of the sample. The charge-discharge cycles for different parts of the sample could be interdependent, masking any periodic behavior. Such a behavior has been seen before in a circuit consisting of two coupled, ac driven relaxation oscillators.¹⁸ In addition to periodic behavior associated with the charge-discharge cycles of each relaxation oscillator, Gollub and co-workers¹⁸ found period-multiplying behavior, similar to the j - x - j and j - x - x patterns we see in Fig. 5, and even nonperiodic behavior for different ac signals applied to their circuit.

In Sec. V, we have shown that, while remaining at a fixed magnetic field, the jumps decrease in magnitude when increasing the temperature, disappearing for $T > 350$ mK. Surprisingly, upon recooling of the sample at fixed magnetic field, the jumps reappeared at low temperatures. This excludes any interpretation that relies on sweeping the magnetic field to establish a nonequilibrium initial condition as a source for the jumps. For example, a series of recent experiments have found that sweeping the magnetic field sets up eddy currents in a 2D layer, which can persist for *days* when it is in the QHS.⁵⁻⁷ In one of these experiments,⁵ a single electron transistor placed close to a single 2D electron layer was used to show that there are sudden jumps in the local Fermi energy associated with these nearly dissipationless eddy currents breaking down the QHS in the 2D layer. Such a breakdown of the QHS, driven by nearly dissipationless eddy currents, could lead to jumps in the probe layer resistance in our experiment. However, by warming the sample to a temperature where neither the jumps nor the hysteretic magnetoresistance are seen, while keeping the magnetic field fixed, we would have allowed the eddy currents to dissipate. Thus, the reappearance of jumps upon recooling of the sample in fixed fields excludes the possibility that eddy currents are responsible for the jumps we see in the probe layer resistance.

The data presented here argue for a different physical origin for the jumps seen in bilayer hole samples. The data show that thermal fluctuations are not responsible for the jumps and it is unlikely that quantum fluctuations are either. Another possibility is that two different energetic requirements are competing against one another to create the jump-relaxation cycle. The data in Ref. 9 show that the time the

system spends in the relaxation part of the cycle increases when increasing the width of the barrier between the two layers, suggesting that the interlayer Coulomb interaction is involved in this part of the cycle. Because the amplitude of the jumps decreases with increasing temperature, along with the strength of the $\nu=1$ QHS, it seems likely that the jump part of the cycle occurs within the QHS layer. The intralayer Coulomb interaction thus likely plays an important role in the jump part of the cycle. We propose that the dynamic competition between the interlayer and intralayer Coulomb interaction in the localized states of the QHS layer creates a charge-discharge cycle, which manifests itself as the relaxation-jump cycle. The capacitive coupling between the probe layer and the localized states of the QHS layer could lead to a charging of the localized states. Thus, the interlayer Coulomb interaction is responsible for charging. Eventually, the localized states in one region of the QHS layer become overcharged compared to neighboring regions, and discharge to them, or, in an avalanche, all the way to the edge state. The intralayer Coulomb interaction is thus responsible for the discharge. The data shown here is consistent with the characteristics of such a charge-discharge cycle. This cycle involves a change in the charge distribution of the QHS layer and, through the interlayer Coulomb interaction, the probe layer as well. The sample itself could contain several such regions, each of which could cycle independently, yielding periodic time evolution, or they could be coupled, yielding complex time evolutions. Finally, at elevated temperatures, the thermal energy would lower the threshold where one region could discharge to neighboring regions, decreasing the amount of excess charge that could build up in any given region.

Ultimately, the physical processes responsible for the jump and the relaxation remain unclear. We emphasize that what *is* clear is that the bulk states of the QHS do not reach equilibrium over extremely long time scales in a wide range of samples. This has been demonstrated clearly by Huels *et al.*⁵ in single layer 2D electron samples, and by us here in bilayer hole samples with barriers larger than 7.5 nm. More broadly, it is possible that the bulk states of the QHS are out of equilibrium in general but that very few experiments are sensitive to the nonequilibrium character of the bulk states. We add that we have been able to identify cases where the bilayer samples do not show any indication of nonequilibrium behavior: in imbalanced bilayer hole samples with barriers smaller than 7.5 nm, we observe no magnetoresistance hysteresis or resistance jumps. This implies that the bulk states of the QHS can reach equilibrium with the probe layer if interlayer tunneling is large enough.

ACKNOWLEDGMENTS

We thank the DOE and Princeton NSF MRSEC for support, and D. A. Huse and A. H. MacDonald for illuminating discussions.

*Present address: Microelectronics Research Center, University of Texas, Austin

- ¹R. E. Prange and S. M. Girvin, *The Quantum Hall Effect* (Springer, New York, 1990).
- ²S. H. Tessmer, P. I. Glicofridis, R. C. Ashoori, L. S. Levitov, and M. R. Melloch, *Nature (London)* **392**, 51 (1998).
- ³S. Ilani, J. Martin, E. Teitelbaum, J. H. Smet, D. Mahalu, V. Umansky, and A. Yacoby, *Nature (London)* **427**, 328 (2004).
- ⁴G. A. Steele, R. C. Ashoori, L. N. Pfeiffer, and K. W. West, *Phys. Rev. Lett.* **95**, 136804 (2005).
- ⁵J. Huels, J. Weis, J. Smet, K. v. Klitzing, and Z. R. Wasilewski, *Phys. Rev. B* **69**, 085319 (2004).
- ⁶M. Pioro-Ladriere, A. Usher, A. S. Sachrajda, J. Lapointe, J. Gupta, Z. Wasilewski, S. Studenikin, and M. Elliott, *Phys. Rev. B* **73**, 075309 (2006).
- ⁷M. Elliott, Y. Lu, K. L. Phillips, W. G. Herrenden-Harker, A. Usher, A. J. Matthews, J. D. Gething, M. Zhu, M. Henini, and D. A. Ritchie, *Europhys. Lett.* **75**, 287 (2006).
- ⁸J. Zhu, H. L. Stormer, L. N. Pfeiffer, K. W. Baldwin, and K. W. West, *Phys. Rev. B* **61**, R13361 (2000).
- ⁹E. Tutuc, R. Pillarisetty, S. Melinte, E. P. DePoortere, and M. Shayegan, *Phys. Rev. B* **68**, 201308(R) (2003).
- ¹⁰W. Pan, J. L. Reno, and J. A. Simmons, *Phys. Rev. B* **71**, 153307 (2005).
- ¹¹A. Siddiki, S. Kraus, and R. R. Gerhardt, *Physica E (Amsterdam)* **34**, 136 (2006).
- ¹²J. P. Eisenstein, L. N. Pfeiffer, and K. W. West, *Appl. Phys. Lett.* **57**, 2324 (1990).
- ¹³N. C. van der Vaart, M. P. de Ruyter van Steveninck, L. P. Kouwenhoven, A. T. Johnson, Y. V. Nazarov, C. J. P. M. Harmans, and C. T. Foxon, *Phys. Rev. Lett.* **73**, 320 (1994).
- ¹⁴N. C. van der Vaart, L. P. Kouwenhoven, M. P. de Ruyter van Steveninck, Y. V. Nazarov, C. J. P. M. Harmans, and C. T. Foxon, *Phys. Rev. B* **55**, 9746 (1997).
- ¹⁵N. G. Kalugin, B. E. Sagol, A. Buss, A. Hirsch, C. Stellmach, G. Hein, and G. Nachtwei, *Phys. Rev. B* **68**, 125313 (2003).
- ¹⁶K. B. Cooper, J. P. Eisenstein, L. N. Pfeiffer, and K. W. West, *Phys. Rev. Lett.* **90**, 226803 (2003).
- ¹⁷G. A. Csathy, D. C. Tsui, L. N. Pfeiffer, and K. W. West, *Phys. Rev. Lett.* **98**, 066805 (2007).
- ¹⁸J. P. Gollub, T. O. Brunner, and B. G. Danly, *Science* **78**, 49 (1978).